

Making the Best of Both Worlds: A Domain-Oriented Transformer for Unsupervised Domain Adaptation

Wenxuan Ma
Beijing Institute of Technology
Beijing, China
wenxuanma@bit.edu.cn

Jinming Zhang
Beijing Institute of Technology
Beijing, China
jinming-zhang@bit.edu.cn

Shuang Li✉
Beijing Institute of Technology
Beijing, China
shuangli@bit.edu.cn

Chi Harold Liu
Beijing Institute of Technology
Beijing, China
liuchi02@gmail.com

Yulin Wang
Tsinghua University
Beijing, China
wang-y119@mails.tsinghua.edu.cn

Wei Li
Inceptio Tech.
Shanghai, China
liweimcc@gmail.com

ABSTRACT

Extensive studies on Unsupervised Domain Adaptation (UDA) have propelled the deployment of deep learning from limited experimental datasets into real-world unconstrained domains. Most UDA approaches align features within a common embedding space and apply a shared classifier for target prediction. However, since a perfectly aligned feature space may not exist when the domain discrepancy is large, these methods suffer from two limitations. First, the coercive domain alignment deteriorates target domain discriminability due to lacking target label supervision. Second, the source-supervised classifier is inevitably biased to source data, thus it may underperform in target domain. To alleviate these issues, we propose to simultaneously conduct feature alignment in two individual spaces focusing on different domains, and create for each space a domain-oriented classifier tailored specifically for that domain. Specifically, we design a Domain-Oriented Transformer (DOT) that has two individual classification tokens to learn different domain-oriented representations, and two classifiers to preserve domain-wise discriminability. Theoretical guaranteed contrastive-based alignment and the source-guided pseudo-label refinement strategy are utilized to explore both domain-invariant and specific information. Comprehensive experiments validate that our method achieves state-of-the-art on several benchmarks. Code is released at <https://github.com/BIT-DA/Domain-Oriented-Transformer>.

CCS CONCEPTS

• **Computing methodologies** → **Image representations**; *Supervised learning by classification*; *Object recognition*.

KEYWORDS

Unsupervised Domain Adaptation, Vision Transformer, Contrastive Learning, Mutual Information

✉:Corresponding author.

Permission to make digital or hard copies of all or part of this work for personal or classroom use is granted without fee provided that copies are not made or distributed for profit or commercial advantage and that copies bear this notice and the full citation on the first page. Copyrights for components of this work owned by others than ACM must be honored. Abstracting with credit is permitted. To copy otherwise, or republish, to post on servers or to redistribute to lists, requires prior specific permission and/or a fee. Request permissions from [permissions@acm.org](https://permissions.acm.org).

MM '22, October 10–14, 2022, Lisboa, Portugal

© 2022 Association for Computing Machinery.

ACM ISBN 978-1-4503-9203-7/22/10...\$15.00

<https://doi.org/10.1145/3503161.3548229>

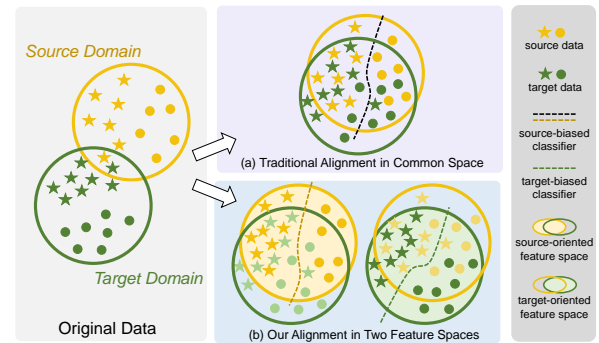


Figure 1: An illustration to show the major difference between classical UDA paradigm and ours. We develop two domain-oriented feature spaces simultaneously to alleviate the discriminability deterioration problem during imperfect domain alignment.

ACM Reference Format:

Wenxuan Ma, Jinming Zhang, Shuang Li✉, Chi Harold Liu, Yulin Wang, and Wei Li. 2022. Making the Best of Both Worlds: A Domain-Oriented Transformer for Unsupervised Domain Adaptation. In *Proceedings of the 30th ACM International Conference on Multimedia (MM '22)*, October 10–14, 2022, Lisboa, Portugal. ACM, New York, NY, USA, 10 pages. <https://doi.org/10.1145/3503161.3548229>

1 INTRODUCTION

There is great interest in the community to deploy deep learning to a variety of multimedia applications, such as media-interpretation [14, 50] and multimodal retrieval [8, 34, 57]. However, deep neural networks heavily rely on large datasets and have inferior generalization ability to data in distinct domains [39, 60]. These problems limit their real-world utility when the data in the target domain are insufficient or sampled from different distributions. To address these practical issues and enhance the models' generalization performance, unsupervised domain adaptation (UDA) is introduced to transfer knowledge from a labeled source domain to another related but unlabeled target domain with the presence of *domain shift* [1, 40] in data distribution.

Over the past decade, researchers have achieved remarkable improvements on UDA. Following the guidance of the theory [1] which shows that the error in target domain is primarily bounded by source error and the domain discrepancy, previous works adopt

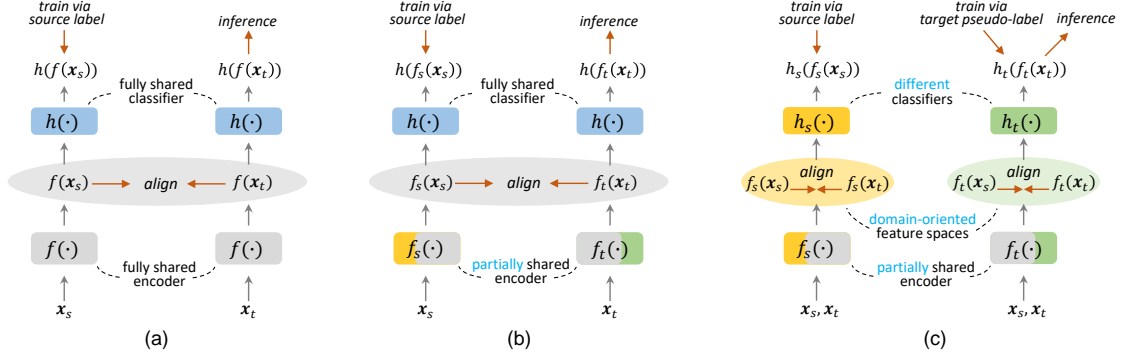


Figure 2: Comparison with the existing UDA paradigms to ours. Most UDA methods follow the classical paradigm (a), which adopts a fully-shared encoder as well as a fully-shared classifier. Features from the two domains are aligned to make the source supervised classifier reusable on target. Some works adopt (b), where partially-shared encoders capture domain-specific information additionally. Utilizing the domain specificity, a feature space with better domain-invariance is created to train a shared classifier on it. Different from them, to maximally retain the target-specific characteristics and facilitate accurate target classification, we propose a new architecture (c). It addresses the discriminability degradation problem during single-space domain alignment by leveraging two domain-oriented feature spaces, each maximally benefits its own domain. Discriminative knowledge transfer and exploitation are then achieved through the target pseudo-label assignment in source-oriented feature space, and the final target classifier trained with target supervision.

a similar paradigm that *learns to extract domain-invariant representations from a shared encoder and builds one shared classifier based on the invariant feature space*, as shown in Fig. 2(a). Specifically, domain-invariant representations are learned via the domain alignment process, which is either in an explicit way like minimizing the difference in statistic measures across two domains [33, 36, 46] or confusing the domain discriminator [15, 35], or implicitly (e.g., conducting self-training on target data [29, 59, 62] or producing target semantic data augmentation [27]). In the ideal scenario, if features from two domains have achieved perfect class-wise alignment, the classifier supervised by source labels can classify target data correctly. However, due to lacking true label supervision in the target domain, the class-discriminative information for target domain is easily jeopardized during the domain alignment process [6], and the shared classifier is inevitably biased to the source domain [29], leading to suboptimal decision boundaries for target data.

Recently, a popular stream of works puts their efforts into incorporating certain domain-specific information to improve the ultimate feature invariance [3, 26, 44], as illustrated in Fig. 2(b). They create domain-specific pathways in the encoder, making it become a partially shared network to better preserve domain-specialized characteristics such as batch statistics [3] or channel activations [26]. These extra features mitigate domain disparity and further improve domain invariance. Although inspiring, the aforementioned methods still follow the paradigm of projecting all the data into a unified domain-invariant feature space. Therefore, when the domain discrepancy is too large for a common space to exist, the same issues such as losing target discriminability and having the classifier source-biased, remain the bottleneck of these approaches.

As the Hungarian mathematician Cornelius Lanczos used to say “*The lack of information cannot be filled with any mathematical tricks*”, the loss in target discriminability during domain alignment should be reduced from the beginning. Therefore, we propose a new paradigm that aims to learn two domain-oriented feature

spaces with different preference in replace of a single one, and propose two distinctly supervised classifiers in replace of a shared one. Specifically, each pair of feature space and classifier has the goal of maximizing the performance of their respective domain by combining cross-domain invariant knowledge and in-domain intrinsic discriminative information. As illustrated in Fig. 2(c), a highly symmetric structure enables target domain to individually possess a maximally discriminative target embedding function and suitable decision boundaries, just as source domain does in previous approaches.

In order to create such two individual feature spaces, we resort to the recent research advances on Vision Transformers (ViTs). The powerful self-attention mechanism enables classification token to adaptively integrate a varying number of image patches, gathering crucial information for recognition [30, 43]. Meanwhile, different class tokens can converge towards dissimilar vectors when trained on different objectives [48]. Thus, the idea of *one token for one domain* raises naturally, which is to deploy two individual class tokens that respectively learn the source-oriented and target-oriented representations. Moreover, we show in the multiple-source DA experiments that creating distinct class tokens for each domain involved is a straightforward and promising extension to our framework.

To be specific, we propose in this paper a Transformer-based UDA framework dubbed as Domain-Oriented Transformer to simultaneously exploit domain-specific and -invariant information in this new DA paradigm. We adopt two class tokens denoted as [src] and [tgt] to learn different mappings and consequently obtain two different feature spaces. In each space, a domain-specific classifier is trained. To maximally preserve the domain-specific information for creating discriminative feature spaces, we let the two classifiers learn from source labels or target pseudo-labels in their respective domain. Also, we put forward a domain-oriented alignment strategy based on supervised contrastive learning [22] and theoretically show that this objective helps representations

in different feature spaces capture correct information from the two original data spaces. Moreover, to improve the quality of target pseudo-labels and promote knowledge transfer from source to target domain, we propose a new label refinement mechanism originating from our dual classifier architecture. Specifically, target data are divided into reliable and unreliable subsets depending on their performance on the noise-free source classifier, and those in the latter subset are assigned new pseudo-labels according to the reliable ones. We empirically show that this method greatly reduces target label noise via utilizing the structural information inside the source data. Our contributions include:

- We propose a new UDA framework that creates two domain-oriented feature spaces for learning different domain-oriented representations. This framework is implemented by creating two classification tokens in a Vision Transformer architecture to integrate different information via self-attention process, together with two individual classifiers.
- We propose a domain-oriented alignment objective in each feature space via contrastive learning with theoretical guarantees, as well as a source-guided pseudo-label refinement process to obtain high-quality target pseudo-labels.
- The performance of our method on three benchmark UDA datasets surpass both CNN-based and ViT-based UDA methods, especially on the most challenging DomainNet.

2 RELATED WORK

2.1 Unsupervised Domain Adaptation (UDA)

To address the performance degradation issue when deploying models to new environments, UDA is proposed and widely studied [60], which aims to train a model that can adapt from a labeled source domain to an unlabeled target domain. The mainstream of UDA methods focuses on learning domain-invariant representations with one shared classifier. To align the source and target features, statistical metrics such as maximum mean discrepancy (MMD) [18] between domains are proposed as objectives for models to minimize [24, 33, 36]. Other approaches find inspiration from adversarial training [17] and thus capture domain-invariant representations via a min-max game with the domain discriminator. For example, DANN [16] introduces a gradient reversal layer to enable simultaneous optimization of the two players. JADA [25] additionally considers class-wise alignment, GVB [9] adds bridge networks to improve alignment process, and RADA [21] enhances the discriminator using dynamic domain labels. However, alignment without the supervision of true target labels will cause target discriminability deterioration [6], since target data from different classes might become closer during the process, posing obstacles for the shared classifier to predict target data correctly.

Recently, some works start to pay more attention to domain-specific information learning [3, 26, 44] for an improved alignment. To model domain discriminative representation separately, DSBN [3] introduces a domain-specific batch normalization mechanism. GDCAN [26] designs a domain conditional attention module in convolutional layers to activate distinctly interested channels for each domain, and DWT [44] makes the domain-specific whitening transform at higher layers. However, these methods still seek to learn a common feature space for a shared classifier, which makes

source domain maintain dominant position in training. Different from them, our method exploits the domain-specific information by creating two different feature spaces, letting both domains simultaneously own a more appropriate mapping for better classification.

Our method is also related to another line of research that borrows the pseudo-labeling idea from semi-supervised learning [23], where the reliable model predictions on unlabeled data are chosen as pseudo-labels to assist the model retraining. Some UDA approaches [5, 10, 62] adopt target pseudo-labels for a better conditional distribution alignment, such as CBST [62] and MSTN [54]. To obtain less noisy pseudo-labels, SHOT [28] and ATDOC [29] leverage the intrinsic structural information of target data to refine the original labels. All these methods can be regarded as conducting implicit domain alignment by making the source and target features of the same class similar, and they also prevent the classifier from behaving overly source-biased. However, these works train both source and target data on the same classifier, which might damage the domain-specific information for both domains. Our method, on the other hand, individually trains two domain-specific classifiers using data and (pseudo-)labels from their respective domains can maximally preserve domain-specific information. Additionally, we propose a source-guided label refinement strategy that to promote knowledge transfer from source to target domain effectively.

2.2 Vision Transformers

Motivated by the significant improvements of Transformers on natural language processing tasks, researchers apply Transformer architectures to computer vision as a potential alternative to CNN backbones. ViT [13] proposes to apply a Transformer encoder with image patches as input to solve image classification problems. Later, DeiT [48] introduces the distillation token and advanced training strategies that enable ViT to effectively train on much smaller datasets. Recent works such as Swin Transformer [32], PVT [51] and CrossViT [4] improve the architecture design from different aspects. Furthermore, other researchers apply Vision Transformers to downstream tasks like semantic segmentation [58, 61], object detection [2, 47] and multimodal tasks [20].

Since Transformer has the intrinsic advantages to extract more transferable representations, several works [55, 56] have been proposed to solve domain adaptation with it. For instance, TransDA [56] injects an attention module after the CNN-based feature extractor to guide the model attention in the source-free UDA setting. TVT [37] applies the domain adversarial training strategy to the classification token as well as the internal transformer blocks. CDTrans [55] also adopts the complete transformer architecture and introduces a cross-attention mechanism between the selected source-target pairs. The outputs of the cross-attention branch are then used to supervise the target self-attention branch. We take a different perspective from these methods by noticing that the ordinary yet particular classification token in Vision Transformers, via self-attention, are capable of capturing most task-related information [30] and learning different mappings, hence are desirable for preserving domain-specific knowledge and learning two differently-oriented feature spaces. Therefore, we propose to train a Transformer with two domain-wise classification tokens, capturing both domain-invariant and specific knowledge for more effective transfer.

3 DOMAIN-ORIENTED TRANSFORMER

In this section, we will introduce our framework in detail. Firstly, we provide a brief review of UDA and the self-attention mechanism in Transformers. Then we describe the key design of two domain-wise class tokens as well as the objective functions that help to learn domain-oriented feature spaces. Finally, a new strategy of target pseudo-label refinement based on this framework is presented.

3.1 Preliminaries

Unsupervised Domain Adaptation (UDA). Contrasting to the assumption of independent and identical distribution, data in UDA is sampled from two different distributions P_s and P_t to form a labeled source domain $\mathcal{D}_s = \{(\mathbf{x}_s^i, y_s^i)\}_{i=1}^{n_s}$ and an unlabeled target domain $\mathcal{D}_t = \{\mathbf{x}_t^j\}_{j=1}^{n_t}$, where n_s and n_t denote the number of training data in each domain. A key in this campaign consists in training a model that performs well on the target domain using knowledge transferred from labeled source data. Opposite to most existing methods encouraging domain alignment within a common feature space, this work turns to extracting different domain-oriented embedding spaces for each domain, allowing both domains to have individual projection that maximally preserves class discriminative knowledge of their own. This is achieved through using the self-attention mechanism within Vision Transformers.

Self-attention. The self-attention mechanism is the core of Vision Transformers [13]. Given a sequence of input token embeddings $X \in \mathbb{R}^{N \times D}$, three learnable linear projectors W_Q , W_K , W_V are applied to the layer-normalized features separately to obtain the queries $Q \in \mathbb{R}^{N \times d}$, keys $K \in \mathbb{R}^{N \times d}$ and the values $V \in \mathbb{R}^{N \times d}$. The query sequence is then matched with the keys to get an $N \times N$ self-attention matrix whose elements represent the semantic relevance of the corresponding query-key pairs. Finally, according to the self-attention matrix, new embeddings are calculated in the form of weighted sums over the values:

$$\text{Attention}(Q, K, V) = \text{softmax}\left(\frac{QK^T}{\sqrt{d}}\right)V. \quad (1)$$

Note that self-attention can be viewed as a selective feature aggregation process at each position, using embeddings from other strongly correlated positions. For the class token, it means the most important representations for recognition will be incorporated [43].

3.2 Learning Domain-Oriented Feature Spaces with Two Domain-Wise Class Tokens

Supervised Losses on Two Class Tokens. Since that the classification token in Transformer is designed to adaptively aggregate patch embeddings, it is suitable for learning domain-oriented feature space. Therefore, we use two class tokens to learn source-oriented embedding function $f_s(\cdot)$ and target-oriented embedding function $f_t(\cdot)$ respectively.

Formally, for each input sequence of image features from image patches $X_p = [\mathbf{x}_p^1; \mathbf{x}_p^2; \dots; \mathbf{x}_p^M] \in \mathbb{R}^{M \times D}$ (which can be either source or target), we add two learnable class tokens [src] and [tgt], namely $X = [\mathbf{x}_{[\text{src}]}; X_p; \mathbf{x}_{[\text{tgt}]}] \in \mathbb{R}^{N \times D}$ where $N = M + 2$. The corresponding two embeddings output by Transformer encoder are regarded as the source-oriented and target-oriented representation of the input image. Therefore, we can obtain four kinds of representations as $f_s(\mathbf{x}_s)$, $f_t(\mathbf{x}_s)$, $f_s(\mathbf{x}_t)$, $f_t(\mathbf{x}_t)$. Next, we will

introduce how to effectively use them for knowledge preservation and transfer.

To begin with, we build a source classifier $h_s(\cdot)$ on $f_s(\cdot)$ and a target classifier $h_t(\cdot)$ on $f_t(\cdot)$. The source labels are then utilized to supervise the source data predictions from source-oriented feature embedding to explore the source-specific information:

$$\mathcal{L}_s^{\text{sup}} = \frac{1}{n_s} \sum_{(\mathbf{x}_s, y_s) \in \mathcal{D}_s} \mathcal{E}(h_s(f_s(\mathbf{x}_s)), y_s), \quad (2)$$

where $\mathcal{E}(\cdot, \cdot)$ denotes the standard cross-entropy (CE) loss. Similarly, the target classifier and the target-oriented features are supervised only by pseudo-labels in the target domain:

$$\mathcal{L}_t^{\text{sup}} = \frac{1}{n_t} \sum_{(\mathbf{x}_t, \hat{y}_t^*) \in \mathcal{D}_t} \mathcal{E}(h_t(f_t(\mathbf{x}_t)), \hat{y}_t^*). \quad (3)$$

Here, \hat{y}_t^* is the one-hot pseudo-label for \mathbf{x}_t . Note that all target training samples are given high-quality pseudo-labels using source knowledge, which we will discuss in § 3.3. Additionally, different from ATDOC [29] which regards a non-parametric model as the auxiliary target classifier to obtain pseudo-labels for training the major classifier, our target classifier is directly trained for target prediction, and it is also used in the final inference stage.

Overall, the supervised loss can be unified as

$$\mathcal{L}^{\text{sup}} = \mathcal{L}_s^{\text{sup}} + \mathcal{L}_t^{\text{sup}}. \quad (4)$$

Domain-Oriented Contrastive Losses. The supervised loss maximally explores domain-specific information in each domain, but the classifiers may end up overfitting. Therefore, information from another domain should be leveraged to improve generalization. However, as aforementioned, indiscriminate alignment within a shared space potentially impairs the class-wise discriminability preserved, making existing methods suboptimal in leveraging the domain specificity.

To address the issue, we propose a pair of contrastive-based domain alignment losses that, with their deployment in different spaces, are theoretically guaranteed to maintain respective domain-specific information beyond feature alignment. Specifically, in source-oriented contrastive loss, for a target sample \mathbf{x}_t^j with pseudo-label \hat{y}_t^{j*} , its positive set consists all source samples with label $y_s = \hat{y}_t^{j*}$. We denote this positive set as $\mathcal{P}_{s,j} = \{\mathbf{x}_s | y_s = \hat{y}_t^{j*}\}$. Then, we have source-oriented contrastive loss for \mathbf{x}_t^j as

$$\mathcal{L}_s^{\text{con}}(\mathbf{x}_t^j) = \frac{-1}{|\mathcal{P}_{s,j}|} \sum_{\mathbf{x}_s^+ \in \mathcal{P}_{s,j}} \left[\log \frac{\exp(\tilde{f}_s(\mathbf{x}_t^j)^\top \tilde{f}_s(\mathbf{x}_s^+)/\tau)}{\sum_{\mathbf{x}_s \in \mathcal{D}_s} \exp(\tilde{f}_s(\mathbf{x}_t^j)^\top \tilde{f}_s(\mathbf{x}_s)/\tau)} \right], \quad (5)$$

where $\tilde{f}_s(\mathbf{x}) = \frac{f_s(\mathbf{x})}{\|f_s(\mathbf{x})\|}$, and the temperature hyper-parameter τ controls the concentration level of the distribution [53]. The total loss $\mathcal{L}_s^{\text{con}}$ is the summation over all target samples.

The symmetric form of Eq. (5) is adopted in target-oriented space, where $\mathcal{P}_{t,i} = \{\mathbf{x}_t | \hat{y}_t^* = y_s^i\}$ represents the positive set for \mathbf{x}_s , and

$$\mathcal{L}_t^{\text{con}}(\mathbf{x}_s^i) = \frac{-1}{|\mathcal{P}_{t,i}|} \sum_{\mathbf{x}_t^+ \in \mathcal{P}_{t,i}} \left[\log \frac{\exp(\tilde{f}_t(\mathbf{x}_s^i)^\top \tilde{f}_t(\mathbf{x}_t^+)/\tau)}{\sum_{\mathbf{x}_t \in \mathcal{D}_t} \exp(\tilde{f}_t(\mathbf{x}_s^i)^\top \tilde{f}_t(\mathbf{x}_t)/\tau)} \right], \quad (6)$$

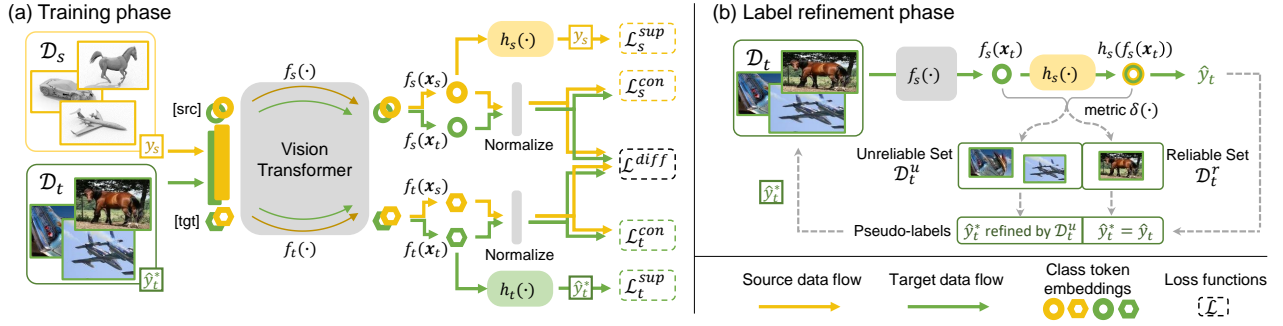


Figure 3: Illustration of the proposed Domain-oriented Transformer framework. (a) In training phase, two domain-wise class tokens ([src] and [tgt]) are simultaneously sent into the Vision Transformer along with image patches to learn different domain-oriented feature embedding functions $f_s(\cdot)$, $f_t(\cdot)$. Two domain-oriented classifiers and specialized learning objectives using source labels and target pseudo-labels are applied to guide them. (b) In the label refinement phase, we utilize a metric function $\delta(\cdot)$ in source-oriented space to divide the target samples into two individual subsets. Pseudo-labels are reassigned to samples of unreliable subset \mathcal{T}_u according to its closest reliable centers.

The target-oriented contrastive loss is summed over the source samples. We combine this pair of losses to obtain the following unified domain alignment objective

$$\mathcal{L}^{con} = \mathcal{L}_s^{con} + \mathcal{L}_t^{con}. \quad (7)$$

Unlike some recent work employing other types of contrastive loss [7], the contrastive loss we proposed is directly related to the mutual information which we seek to maximize.

Remark The following two inequalities reveal the relationship between domain-oriented contrastive losses and two specific mutual information. For simplicity, we denote the random variable for representations $f_s(\mathbf{x}_d)$, $f_t(\mathbf{x}_d)$ as f_s^d , f_t^d , $d \in \{s, t\}$, and have:

$$-\mathcal{L}_s^{con} \leq I(f_s^s; f_s^t, y) + \log(N - 1) \\ = I(f_s^s; f_s^t) + I(f_s^s; y | f_s^t) + \log(N - 1) \quad (8)$$

$$-\mathcal{L}_t^{con} \leq I(f_t^t; f_t^s, y) + \log(N - 1) \\ = I(f_t^t; f_t^s) + I(f_t^t; y | f_t^s) + \log(N - 1) \quad (9)$$

Above inequalities show that both losses encourages feature alignment between source and target. Moreover, minimizing source-oriented contrastive loss also maximizes source-specific information for representation $f_s(\cdot)$, while minimizing target-oriented contrastive loss, on the other hand, maximizes target-specific information for representation $f_t(\cdot)$. We give the proofs in the supplementary.

Regularization on Representation Difference. The above losses are expected to provide different domain-specific knowledge for respective domains. Therefore, two learned domain-oriented representations for the same input should be distinctive. To explicitly promote this and accelerate the training, we add a regularization term to penalize the similar pair of representations. In this way, source-oriented features space explores more source-specific information and becomes more beneficial for source classification, while the target-oriented space is the opposite, making the best of both domains. This regularization term takes the following form:

$$\mathcal{L}^{diff} = \frac{1}{n_s + n_t} \sum_{\mathbf{x} \in \mathcal{D}_s \cup \mathcal{D}_t} \left(\frac{\tilde{f}_s(\mathbf{x})^\top \tilde{f}_t(\mathbf{x})}{\|\tilde{f}_s(\mathbf{x})\| \|\tilde{f}_t(\mathbf{x})\|} \right)^2 \quad (10)$$

3.3 Target Pseudo-label Refinement

Similar to self-training based UDA methods [28, 59], our objective functions also rely on the quality of target pseudo-labels. In previous methods, once the shared classifier is trained by noisy pseudo-labels, it may remember its false label and produce overconfident predictions [38], making the subsequent refinement hard to improve. To better exploit the advantage of our symmetric structure, we propose a new label refinement strategy to reduce the noise from original predictions. Our insight here is that the source-oriented feature space and classifier, not being supervised by target pseudo-labels, are less affected by the previous noisy pseudo-labels. Accordingly, they can serve as fair judges to determine whether a target sample is currently well-aligned or not. Hereafter, by evaluating target samples in the source-oriented feature space, we are capable of largely reducing overconfident errors.

To be precise, we evaluate all target samples by a metric $\delta(\cdot)$ and accordingly divide them into reliable target subset \mathcal{D}_t^r and unreliable target subset \mathcal{D}_t^u . On one hand, samples in the former set are considered to be easy to transfer or well aligned with source domain, thus we trust their predictions and use them directly as pseudo-labels. On the other hand, we reassign pseudo-labels for samples in the unreliable set according to their nearest reliable center in order to keep the pseudo-labels uniform within the neighborhood. During the training procedure, we iteratively conduct label refinement until the network converges.

In summary, the procedure of target pseudo-label refinement is as follows. First, the initial predictions for target samples on source-specific classifier are

$$\hat{y}_t = \arg \max_{k=1, \dots, K} \mathbf{p}^{(k)} = \arg \max_{k=1, \dots, K} \sigma^{(k)}(h_s(f_s(\mathbf{x}_t))), \quad (11)$$

where $\sigma^{(k)}(\mathbf{a}) = \frac{\exp(a^k)}{\sum_j \exp(a^j)}$ and K is the number of categories. Next, we denote $\mathbf{x}_{t,k}$ to be all the target samples with prediction $\hat{y}_t = k$ and construct class-wise reliable set $\mathcal{D}_t^r = \bigcup_k \mathcal{D}_{t,k}^r$, where $\mathcal{D}_{t,k}^r = \{\mathbf{x}_t | \mathbf{x}_t \in \mathbf{x}_{t,k}, \delta(\mathbf{x}_t) \geq \overline{\delta(\mathbf{x}_{t,k})}\}$ while the rest go to unreliable set \mathcal{D}_t^u . Then, K reliable class centers are calculated, and the refined pseudo-labels are obtained by finding the nearest class center:

Table 1: Accuracy (%) on DomainNet for unsupervised domain adaption. The column-wise domains are selected as the source domain and the row-wise domains as the target domain. CNN-based methods are presented in the supplementary.

ViT-S [13]	clp	inf	pnt	qdr	rel	skt	Avg.	CDTrans-S [55]	clp	inf	pnt	qdr	rel	skt	Avg.	DOT-S	clp	inf	pnt	qdr	rel	skt	Avg.
clp	-	19.3	43.2	14.3	58.8	46.4	36.4	clp	-	24.2	47.0	22.3	64.3	50.6	41.7	clp	-	19.5	51.3	27.5	67.6	51.7	43.5
inf	35.2	-	36.7	4.7	50.4	30.0	31.4	inf	45.3	-	45.3	6.6	62.8	38.3	39.7	inf	59.5	-	51.5	14.2	69.9	46.8	48.4
pnt	44.7	18.7	-	4.5	59.0	38.1	33.0	pnt	53.6	20.4	-	10.6	63.9	42.4	38.2	pnt	58.5	18.9	-	16.5	70.4	47.2	42.3
qdr	23.2	3.3	10.1	-	17.0	14.5	13.6	qdr	2.8	0.2	0.6	-	0.7	4.2	1.7	qdr	39.3	6.1	22.3	-	34.7	25.6	25.6
rel	48.3	18.9	50.4	7.0	-	37.0	32.3	rel	47.1	17.9	45.0	7.9	-	31.7	29.9	rel	62.3	20.0	57.0	20.9	-	49.4	41.9
skt	54.3	16.5	41.1	15.3	53.8	-	36.2	skt	61.0	19.3	46.8	22.8	59.2	-	41.8	skt	64.6	16.8	49.9	30.4	65.4	-	45.4
Avg.	41.1	15.3	36.3	9.2	47.8	33.2	30.5	Avg.	42.0	16.4	36.9	14.0	50.2	33.4	32.2	Avg.	56.8	16.3	46.4	21.9	61.6	44.1	41.2
ViT-B[13]	clp	inf	pnt	qdr	rel	skt	Avg.	CDTrans-B[55]	clp	inf	pnt	qdr	rel	skt	Avg.	DOT-B	clp	inf	pnt	qdr	rel	skt	Avg.
clp	-	20.1	46.2	13.0	62.3	48.8	38.1	clp	-	27.9	57.6	27.9	73.0	58.8	49.0	clp	-	20.2	53.6	26.7	71.2	55.2	45.4
inf	46.4	-	45.2	5.1	62.3	37.5	39.3	inf	58.6	-	53.4	9.6	71.1	47.6	48.1	inf	63.0	-	54.6	12.3	73.1	50.7	50.7
pnt	48.1	19.1	-	4.4	62.5	41.8	35.2	pnt	60.7	24.0	-	13.0	69.8	49.6	43.4	pnt	61.8	20.3	-	11.4	72.2	50.5	43.2
qdr	28.2	5.2	14.4	-	21.9	17.7	17.5	qdr	2.9	0.4	0.3	-	0.7	4.7	1.8	qdr	47.3	7.4	30.3	-	44.6	33.7	32.7
rel	53.2	19.3	53.5	7.2	-	41.6	35.0	rel	49.3	18.7	47.8	9.4	-	33.5	31.7	rel	62.9	20.0	56.9	17.3	-	49.3	41.3
skt	58.0	18.5	46.5	15.7	58.7	-	39.5	skt	66.8	23.7	54.6	27.5	68.0	-	48.1	skt	67.3	18.7	52.9	27.8	69.8	-	47.3
Avg.	46.8	16.4	41.2	9.1	53.5	37.5	34.1	Avg.	47.7	18.9	42.7	17.5	56.5	38.8	37.0	Avg.	60.5	17.3	49.7	19.1	66.2	47.9	43.4

$$c_k = \frac{1}{|\mathcal{D}_{t,k}^r|} \sum_{\mathbf{x}_t \in \mathcal{D}_{t,k}^r} f_s(\mathbf{x}_t). \quad (12)$$

$$\hat{y}_t^* = \begin{cases} \hat{y}_t & \text{if } \mathbf{x}_t \in \mathcal{D}_t^r, \\ \arg \min_k w_k \cdot d(f_s(\mathbf{x}_t), c_k) & \text{if } \mathbf{x}_t \in \mathcal{D}_t^u. \end{cases} \quad (13)$$

Here, $d(\cdot, \cdot)$ denotes the distance measure where we use cosine distance, and $w_k = \exp(\frac{|\mathcal{D}_{t,k}^r|}{|\mathcal{D}_t^r|})$ is a class-wise distance weight related to the size of each class-wise reliable subset. It is based on the consideration that easier-to-transfer categories produce more reliable samples and they also tend to form more compact clusters, therefore samples with equal distance to several class centers are more likely belong to the cluster having less reliable samples.

Finally, we discuss the choices of the metric function $\delta(\cdot)$. As it should return higher values for more reliable samples, we consider confidence score, entropy and negative energy [31] as options. The three metrics can be calculated as

$$\text{Confidence: } \delta_{conf}(\mathbf{x}_t) = \max_k \mathbf{p}^{(k)}, \quad (14)$$

$$\text{Entropy: } \delta_{ent}(\mathbf{x}_t) = - \sum_k \mathbf{p}^{(k)} \log \mathbf{p}^{(k)}, \quad (15)$$

$$\text{Energy: } \delta_{energy}(\mathbf{x}_t) = \log \sum_k \exp(h_s(f_s(\mathbf{x}_t))^{(k)}). \quad (16)$$

Experimentally, δ_{energy} is the optimal choice. To be clear, we summarize the overall label refinement procedure in Alg. 1.

Algorithm 1 Algorithm of Target Pseudo-label Refinement.

Input: Source-oriented target features $f_s(\mathbf{x}_t)$; Source-oriented classifier h_s ; Metric function $\delta(\cdot)$; category number K

Output: Refined target pseudo-labels \hat{y}_t^*

- 1: Obtain initial pseudo-labels \hat{y}_t by Eq. (11);
- 2: **for** $k = 1$ to K **do**
- 3: Calculate $\delta(\mathbf{x}_{t,k})$ by averaging $\delta(\mathbf{x}_t)$ which has $\hat{y}_t = k$;
- 4: Select \mathbf{x}_t, \hat{y}_t with $\delta(\mathbf{x}_t) \geq \delta(\mathbf{x}_{t,k})$ into class-wise reliable set $\mathcal{D}_{t,k}^r$;
- 5: Obtain reliable class center c_k by Eq. (12);
- 6: **end for**
- 7: Combine all $\mathcal{D}_{t,k}^r$ to \mathcal{D}_t^r , put the rest target into unreliable set \mathcal{D}_t^u ;
- 8: Obtain refined target pseudo-labels \hat{y}_t^* by Eq. (13).

3.4 Overall Formulation

In summary, our objective is the sum of losses with two trade-off parameters λ and β :

$$\mathcal{L}_{DOT} = \mathcal{L}^{sup} + \lambda \mathcal{L}^{con} + \beta \mathcal{L}^{diff}. \quad (17)$$

As illustrated in Fig. 3, this highly symmetric architecture learns two domain-oriented feature embedding function and two domain-oriented classifier, enabling a simultaneous exploitation for domain-wise discrimination knowledge and domain-invariant information.

4 EXPERIMENTS

4.1 Datasets and Setup

We test and analyze our proposed method on three benchmark datasets in UDA, namely Office-Home [49], VisDA-2017 [42] and DomainNet [41]. We construct transfer tasks on them following the standard procedure. Detailed descriptions about these datasets and task constructions can be found in the supplementary. Note that unless otherwise specified, all the reported accuracies of target domain come from the target classifier prediction $h_t(f_t(\mathbf{x}_t))$.

4.2 Implementation Details

We adopt ViT-Small (S) and ViT-Base (B) [13] pretrained on ImageNet-1k [11] (DeiT [48] pretrained model) as backbones. We set the base learning rate as 1e-3 on VisDA2017 and DomainNet, while using 3e-4 on Office-Home. Both classifiers are the single fully-connect layer that are randomly initialized and have a 10 times larger learning rate following [25]. The model is optimized by SGD with momentum 0.9 and weight decay 1e-3. The batch-size is 32 for both domains. The initial target pseudo-labels are obtained from the source model while we update these pseudo-labels throughout the training. The trade-off parameters λ and β in Eq. (17) are set as 1.0 and 0.1 respectively, and the temperature τ is 0.07 for all datasets.

4.3 Overall Results

We compare our DOT to various UDA methods using ResNet-50/101 or ViT-S/B as the backbones in the experiments. We mark the pretrained dataset as well as parameter size for each model.

The results on DomainNet are shown in Table 1, where strong results validate DOT's effectiveness in challenging transfer tasks and unseen target test data. We observe that DOT-S outperforms

Table 2: Accuracy (%) on VisDA-2017 for unsupervised domain adaption. (IN-1k/21k denotes the pretrained model on ImageNet-1k/21k, and ~ denotes the method having similar amount of parameters to the corresponding backbone.)

Method	Pretrained	Params (M)	plane	bcycl	bus	car	horse	knife	mcycl	person	plant	sktbrd	train	truck	Avg.
ResNet-101 [19]		44.6	55.1	53.3	61.9	59.1	80.6	17.9	79.7	31.2	81.0	26.5	73.5	8.5	52.4
+ JADA [25]	IN-1k	~	91.9	78.0	81.5	68.7	90.2	84.1	84.0	73.6	88.2	67.2	79.0	38.0	77.0
+ IC ² FA [12]	IN-1k	~	89.7	70.6	79.8	84.3	96.5	72.1	90.4	65.3	92.7	63.3	86.5	36.0	77.3
+ DSBN [3]	IN-1k	~	94.7	86.7	76.0	72.0	95.2	75.1	87.9	81.3	91.1	68.9	88.3	45.5	80.2
ViT-S [13]		21.8	95.7	46.3	82.9	68.7	83.4	57.1	96.3	21.8	87.5	42.8	92.8	24.7	66.7
+ DOT-S (ours)	IN-1k	~	97.8	89.7	89.8	84.9	97.2	95.8	93.2	84.6	96.3	91.1	91.3	60.0	89.3
ViT-B		86.3	97.7	48.1	86.6	61.6	78.1	63.4	94.7	10.3	87.7	47.7	94.4	35.5	67.1
+ TVT-B [37]	IN-21k	~	92.9	85.6	77.5	60.5	93.6	98.2	89.4	76.4	93.6	92.0	91.7	55.7	83.9
+ TVT-B [37]	IN-1k	~	-	-	-	-	-	-	-	-	-	-	-	-	85.1
+ CDTrans-B [55]	IN-1k	~	97.1	90.5	82.4	77.5	96.6	96.1	93.6	88.6	97.9	86.9	90.3	62.8	88.4
+ DOT-B (ours)	IN-1k	~	99.3	92.7	89.0	78.8	98.2	96.1	93.1	80.2	97.6	95.8	94.4	69.0	90.3

Table 3: Accuracy (%) on Office-Home for unsupervised domain adaption.

Method	Pretrained	Params (M)	Ar→Cl	Ar→Pr	Ar→Re	Cl→Ar	Cl→Pr	Cl→Re	Pr→Ar	Pr→Cl	Pr→Re	Re→Ar	Re→Cl	Re→Pr	Avg.
ResNet-50 [19]		25.6	44.9	66.3	74.3	51.8	61.9	63.6	52.4	39.1	71.2	63.8	45.9	77.2	59.4
+ GDCAN [26]	IN-1k	~	57.3	75.7	83.1	68.6	73.2	77.3	66.7	56.4	82.2	74.1	60.7	83.0	71.5
+ ATDOC [29]	IN-1k	~	58.3	78.8	82.3	69.4	78.2	78.2	67.1	56.0	82.7	72.0	58.2	85.5	72.2
+ TCL [7]	IN-1k	~	59.4	78.8	81.6	69.9	76.9	78.9	69.2	58.7	82.4	76.9	62.7	85.6	73.4
ViT-S [13]		21.8	54.4	73.8	79.9	68.6	72.6	75.1	63.6	50.2	80.0	73.6	55.2	82.2	69.1
+ CDTrans-S [55]	IN-1k	~	60.6	79.5	82.4	75.6	81.0	82.3	72.5	56.7	84.4	77.0	59.1	85.5	74.7
+ DOT-S (ours)	IN-1k	~	63.7	82.2	84.3	74.9	84.3	83.0	72.4	61.0	84.8	76.4	64.1	86.7	76.5
ViT-B		86.3	60.2	78.3	82.7	73.3	77.3	80.3	69.6	54.9	82.3	77.3	59.9	85.2	73.4
+ TVT-B [37]	IN-1k	~	-	-	-	-	-	-	-	-	-	-	-	-	78.9
+ TVT-B [37]	IN-21k	~	74.9	86.8	89.5	82.8	88.0	88.3	79.8	71.9	90.1	85.5	74.6	90.6	83.6
+ CDTrans-B [55]	IN-1k	~	68.8	85.0	86.9	81.5	87.1	87.3	79.6	63.3	88.2	82.0	66.0	90.6	80.5
+ DOT-B (ours)	IN-1k	~	69.0	85.6	87.0	80.0	85.2	86.4	78.2	65.4	87.9	79.7	67.3	89.3	80.1
+ DOT-B (ours)	IN-21k	~	73.1	89.1	90.1	85.5	89.4	89.6	83.2	72.1	90.4	84.4	72.9	91.5	84.3

Table 4: Ablation studies on different components of our method on the Office-Home dataset with ViT-S.

Method	\mathcal{L}^{sup}	\mathcal{L}^{con}	\mathcal{L}^{diff}	Ar→Cl	Ar→Pr	Ar→Re	Cl→Ar	Cl→Pr	Cl→Re	Pr→Ar	Pr→Cl	Pr→Re	Re→Ar	Re→Cl	Re→Pr	Avg.
ViT-S	\mathcal{L}_s^{sup}	-	-	54.4	73.8	79.9	68.6	72.6	75.1	63.6	50.2	80.0	73.6	55.2	82.2	69.1
DOT-S	✓	-	-	61.3	80.2	83.0	71.4	81.9	81.8	69.8	58.4	84.9	75.7	61.4	85.9	74.6
	✓	✓	-	64.2	82.4	84.3	74.6	83.4	82.4	72.3	60.7	85.0	76.3	63.0	86.0	76.2
	✓	✓	✓	63.7	82.2	84.3	74.9	84.3	83.0	72.4	61.0	84.8	76.4	64.1	86.7	76.5

CDTrans on average by 9.0%. Out of a total 30 tasks, DOT-S surpasses CDTrans-S on 28 of them by a large margin, especially when the source domain is *Quickdraw*. The significant accuracy boost on these unseen test data proves that our target-oriented classifier, though trained with target samples only, learns to generalize well and will not easily overfit to noisy pseudo-labels. Moreover, our method achieves satisfying results when transferring to *Real* domain, achieving an average of 61.6% and 66.2% with DOT-S/B.

Results on VisDA-2017 and Office-Home are reported in Table 2 and 3. We notice that DOT-B achieves a class average accuracy of 90.1% on VisDA-2017, which outperforms all the baseline methods, including DSBN which explores domain-specific information via batch statistics. On Office-Home, our method also achieves competitive results: DOT (IN-1k) outperforms TVT (IN-1k) by 1.2% on average and DOT (IN-21k) outperforms TVT (IN-21k) by 0.7%. These results validate the effectiveness of both our proposed strategies and the Transformer backbone on UDA.

4.4 Insight Analysis

In this section, we carry out experiments to fully investigate the influence of each component in our Domain-Oriented Transformer. All the analytical experiments are conducted based on DOT-S.

4.4.1 Ablation Study and Sensitivity Analysis. To verify that each term in the loss function contributes to our method, we conduct an ablation study as shown in Table 4. We observe that the performance improves with \mathcal{L}^{sup} exploring the target-specific information, and

\mathcal{L}^{con} promoting cross-domain knowledge transfer as well as \mathcal{L}^{diff} increasing the difference between domain-oriented spaces.

To show that our method is robust to different choices on hyperparameters λ and β , we vary their values within a certain range and test their performance on Office-Home using different combinations. The average result is demonstrated in Fig. 4(a). We see that DOT maintains a stable performance over a wide range of choices.

4.4.2 On Contrastive-based Domain Alignment.

Comparison of Domain Alignment Methods. As shown in Table 5a, we conduct experiments on different alternatives for the domain alignment loss \mathcal{L}^{con} . These alternatives includes: *Maximum Mean Discrepancy (MMD)* [18], a classic statistic-based metric, *Domain adversarial training (DANN)* [15] that utilizes the domain discriminator, and *Transferrable Contrastive Loss (TCL)* [7], another contrastive-based method. We observe that our contrastive alignment objective outperforms all other variants, since it encourages not only the feature alignment, but also the maximization of domain-specific information that is relevant to the task.

Contrastive-based Alignment Improves Generalization. We further investigate the effect of contrastive-based domain alignment in terms of generalization ability. We test target data accuracy on source-specific classifier, (i.e. $h_s(f_s(x_t))$) and vice versa ($h_t(f_t(x_s))$). Note that the test data comes from the other domain, and therefore is never trained on the classifier being tested. As shown in Fig. 4(b), after applying contrastive losses (denote as w/ \mathcal{L}^{con}), the prediction accuracies on unseen data from the other

Table 5: Comparison results between different variants of DOT on Office-Home dataset. Results are averaged on all 12 tasks.

(a) Comparison of alignment methods.			(b) Comparison of pseudo-labeling methods.			(c) Comparison of metric function $\delta(\cdot)$.				
Variant	Method	Acc.	Variant	Method	Acc.	Variant	Method	\mathcal{T}_r acc.	\mathcal{T}_r ratio	Acc.
Alignment Methods	w/ MMD [18]	75.5	Pseudo-labeling Methods	w/ Confidence	72.6	Metric Function	δ_{conf}	85.7	59.2	75.5
	w/ DANN [15]	74.9		w/ CBST [62]	73.7		δ_{ent}	84.8	58.3	75.4
	w/ TCL [7]	76.3		w/ SHOT [28]	76.2		δ_{energy}	87.5	53.6	76.5
	w/ <i>ours</i>	76.5		w/ <i>ours</i>	76.5					

Table 6: Label refinement within different feature space of our method on the Office-Home dataset with ViT-S.

Feature space	Ar→Cl	Ar→Pr	Ar→Re	Cl→Ar	Cl→Pr	Cl→Re	Pr→Ar	Pr→Cl	Pr→Re	Re→Ar	Re→Cl	Re→Pr	Avg.
Target-oriented $f_t(x_t)$	61.7	81.6	84.2	73.5	81.1	82.8	69.6	54.5	84.5	76.1	58.1	85.5	74.4
Source-oriented $f_s(x_t)$	63.7	82.2	84.3	74.9	84.3	83.0	72.4	61.0	84.8	76.4	64.1	86.7	76.5

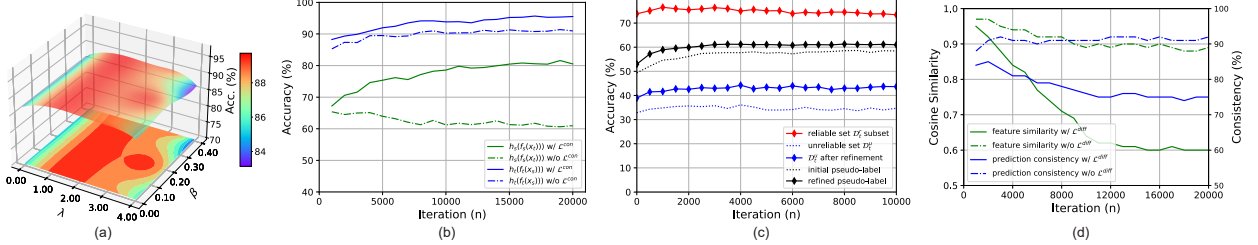


Figure 4: Analysis experiments: (a) Parameter sensitivity analysis on Office-Home, (b) Improvements on generalization brought by contrastive-based Alignment on Visda-2017, (c) Development in target pseudo-label accuracy during training process on Office-Home (Pr → Cl) (d) Development in difference between class tokens during training process on DomainNet (clp → skt).

domain improve significantly, verifying that the alignment process help both feature spaces learn more invariant and robust embeddings. We can also see that without contrastive losses, the accuracy of $h_s(f_s(x_t))$ decreases, indicating the occurrence of overfitting.

4.4.3 On Pseudo-label Refinement.

Comparison to existing pseudo-labeling methods. Table 5b demonstrates the results of DOT-S on Office-Home using different pseudo-labeling methods, including selection-based methods [62] and refinement-based methods [28]. Note that our strategy can be viewed as a combination of the two. The results prove that our label-refinement strategy works better. Fig. 4(c) illustrates how it operates. The reliable subset includes high-quality pseudo-labels, and noisy labels in unreliable subset are reduced after label reassignment, bringing an overall improvement in label quality.

Comparison of metrics for selecting reliable target. In Table 5c we compare different metric functions. We report the average of target pseudo-label accuracy, as well as the sample ratio (i.e. $|\mathcal{D}_t^r|/n_t$) of the reliable set over all 12 tasks during the first selection process. We observe that δ_{energy} selects the reliable subset with the least amount of noise and helps the model achieve top performance.

Which Feature Space for Label Refinement? To prove that the label refinement process achieves better results when utilizing source-oriented representation instead of target-oriented ones, we compare the two variants on Office-Home. Specifically, we employ the same label refinement strategy on $f_s(x_t)$ and $f_t(x_t)$ respectively and use the obtained pseudo-labels for model training. The results are listed in Table. 6, which indicates that source-oriented representation is more suitable, especially for harder transfer tasks like Pr→Cl when pseudo-labels before refinement are noisier. We think this improvement is brought by leveraging source knowledge.

Table 7: Multi-source domain adaptation on Office-Home.

Method	Cl,Pr,Re → Ar	Ar,Pr,Re → Cl	Ar,Cl,Re → Pr	Ar,Cl,Pr → Re	Avg.
ResNet-50	49.3	46.9	66.5	73.6	59.1
+ DARN [52]	69.9	68.6	83.4	84.3	76.5
+ WADN [45]	73.8	70.2	86.3	87.3	79.4
ViT-S	75.9	59.9	82.2	83.4	75.4
+ DOT-S (<i>ours</i>)	79.4	65.6	87.1	87.6	79.9

4.4.4 On Discrepancy of token embeddings. Fig. 4(d) shows the trend of feature similarity (measured by cosine similarity and prediction consistency using the same classifier h_t) with training. The results validate that the difference between two domain-oriented feature spaces represented by [src] and [tgt] token embeddings increases through training, and \mathcal{L}^{diff} prompts it significantly.

4.5 Extension to the Multi-Source Domain Adaptation Setting

We show that the idea of one class token for one domain can be naturally extended to multiple source setting. Specifically, we create the same amount of domain tokens to the total number of domains. As reported in Table 7, we show that based on a strong performance of ViT-S baseline, DOT outperforms WADN by 0.5% in average.

5 CONCLUSION

We propose Domain-Oriented Transformer for UDA. Different from the classical UDA paradigm that learns a domain-invariant representation and a shared classifier, we propose to simultaneously learn two embedding spaces and two classifiers via class tokens in Vision Transformer. Our new paradigm enables the simultaneous exploitation of domain-specific and -invariant information. We propose contrastive alignment losses and source-guided label refinement to promote cross-domain knowledge transfer, and validates their effectiveness on three benchmarks.

ACKNOWLEDGEMENTS

This paper was supported by National Key R&D Program of China (No. 2021YFB3301503), and also supported by the National Natural Science Foundation of China (No. 11727801).

REFERENCES

- [1] Shai Bendavid, John Blitzer, Koby Crammer, Alex Kulesza, Fernando Pereira, and Jennifer Wortman Vaughan. 2010. A theory of learning from different domains. *MLJ* 79, 1-2 (2010), 151–175.
- [2] Nicolas Carion, Francisco Massa, Gabriel Synnaeve, Nicolas Usunier, Alexander Kirillov, and Sergey Zagoruyko. 2020. End-to-end object detection with transformers. In *ECCV*. 213–229.
- [3] Woong-Gi Chang, Tackgeun You, Seonguk Seo, Suha Kwak, and Bohyung Han. 2019. Domain-Specific Batch Normalization for Unsupervised Domain Adaptation. In *CVPR*. 7354–7362.
- [4] Chun-Fu Chen, Quanfu Fan, and Rameswar Panda. 2021. Crossvit: Cross-attention multi-scale vision transformer for image classification. In *ICCV*. 357–366.
- [5] Minghao Chen, Shuai Zhao, Haifeng Liu, and Deng Cai. 2020. Adversarial-learned loss for domain adaptation. In *AAAI*. 3521–3528.
- [6] Xinyang Chen, Sinan Wang, Mingsheng Long, and Jiamin Wang. 2019. Transferability vs. Discriminability: Batch Spectral Penalization for Adversarial Domain Adaptation. In *ICML*. 1081–1090.
- [7] Yang Chen, Yingwei Pan, Yu Wang, Ting Yao, Xinmei Tian, and Tao Mei. 2021. Transferrable Contrastive Learning for Visual Domain Adaptation. In *MM*. 3399–3408.
- [8] Tai-Te Chu, Chia-Chun Chang, An-Zi Yen, Hen-Hsen Huang, and Hsin-Hsi Chen. 2020. Multimodal retrieval through relations between subjects and objects in lifelog images. In *LSC Workshops*. 51–55.
- [9] Shuhao Cui, Shuhui Wang, Junbao Zhuo, Chi Su, Qingming Huang, and Qi Tian. 2020. Gradually Vanishing Bridge for Adversarial Domain Adaptation. In *CVPR*. 12455–12464.
- [10] Debansmit Das and CS Lee. 2018. Graph matching and pseudo-label guided deep unsupervised domain adaptation. In *ICANN*. 342–352.
- [11] Jia Deng, Wei Dong, Richard Socher, Li-Jia Li, Kai Li, and Li Fei-Fei. 2009. Imagenet: A large-scale hierarchical image database. In *CVPR*. 248–255.
- [12] Wanxia Deng, Yawen Cui, Zhen Liu, Gangyao Kuang, Dewen Hu, Matti Pietikäinen, and Li Liu. 2021. Informative Class-Conditioned Feature Alignment for Unsupervised Domain Adaptation. In *MM*. 1303–1312.
- [13] Alexey Dosovitskiy, Lucas Beyer, Alexander Kolesnikov, Dirk Weissenborn, Xiuhua Zhai, Thomas Unterthiner, Mostafa Dehghani, Matthias Minderer, Georg Heigold, Sylvain Gelly, et al. 2020. An Image is Worth 16x16 Words: Transformers for Image Recognition at Scale. In *ICLR*.
- [14] Thomas Forgiione, Axel Carlier, Géraldine Morin, Wei Tsang Ooi, Vincent Charvillat, and Praveen Kumar Yadav. 2018. An implementation of a dash client for browsing networked virtual environment. In *MM*. 1263–1264.
- [15] Yaroslav Ganin and Victor Lempitsky. 2015. Unsupervised domain adaptation by backpropagation. In *ICML*. 1180–1189.
- [16] Yaroslav Ganin and Victor Lempitsky. 2015. Unsupervised Domain Adaptation by Backpropagation. In *ICML*. 1180–1189.
- [17] Ian Goodfellow, Jean Pouget-Abadie, Mehdi Mirza, Bing Xu, David Warde-Farley, Sherjil Ozair, Aaron Courville, and Yoshua Bengio. 2014. Generative adversarial nets. In *NeurIPS*. 2672–2680.
- [18] Arthur Gretton, Karsten M Borgwardt, Malte Rasch, Bernhard Schölkopf, and Alex J Smola. 2007. A kernel method for the two-sample-problem. In *NeurIPS*. 513–520.
- [19] Kaiming He, Xiangyu Zhang, Shaoqing Ren, and Jian Sun. 2016. Deep residual learning for image recognition. In *CVPR*. 770–778.
- [20] Ronghang Hu and Amanpreet Singh. 2021. UniT: Multimodal Multitask Learning with a Unified Transformer. In *ICCV*. 1439–1449.
- [21] Xin Jin, Cuiling Lan, Wenjun Zeng, and Zhibo Chen. 2021. Re-energizing Domain Discriminator with Sample Relabeling for Adversarial Domain Adaptation. In *ICCV*. 9174–9183.
- [22] Prannay Khosla, Piotr Teterwak, Chen Wang, Aaron Sarna, Yonglong Tian, Phillip Isola, Aaron Maschinot, Ce Liu, and Dilip Krishnan. 2020. Supervised contrastive learning. In *NeurIPS*.
- [23] Dong-Hyun Lee et al. 2013. Pseudo-label: The simple and efficient semi-supervised learning method for deep neural networks. In *ICML Workshops*, Vol. 3. 896.
- [24] Shuang Li, Chi Harold Liu, Qixia Lin, Qi Wen, Limin Su, Gao Huang, and Zhengming Ding. 2020. Deep Residual Correction Network for Partial Domain Adaptation. *TPAMI* (2020), 1–1.
- [25] Shuang Li, Chi Harold Liu, Binhui Xie, Limin Su, Zhengming Ding, and Gao Huang. 2019. Joint Adversarial Domain Adaptation. In *MM*. 729–737.
- [26] Shuang Li, Binhui Xie, Qixia Lin, Chi Harold Liu, Gao Huang, and Guoren Wang. 2021. Generalized Domain Conditioned Adaptation Network. *TPAMI* (2021).
- [27] Shuang Li, Mixue Xie, Kaixiong Gong, Chi Harold Liu, Yulin Wang, and Wei Li. 2021. Transferable Semantic Augmentation for Domain Adaptation. In *CVPR*. 11516–11525.
- [28] Jian Liang, Dapeng Hu, and Jiashi Feng. 2020. Do we really need to access the source data? source hypothesis transfer for unsupervised domain adaptation. In *ICML*. 6028–6039.
- [29] Jian Liang, Dapeng Hu, and Jiashi Feng. 2021. Domain Adaptation with Auxiliary Target Domain-Oriented Classifier. In *CVPR*. 16632–16642.
- [30] Youwei Liang, GE Chongjian, Zhan Tong, Yibing Song, Jue Wang, and Pengtao Xie. 2022. EViT: Expediting Vision Transformers via Token Reorganizations. In *ICLR*.
- [31] Weitang Liu, Xiaoyun Wang, John Owens, and Yixuan Li. 2020. Energy-based out-of-distribution detection. *NeurIPS* 33 (2020), 21464–21475.
- [32] Ze Liu, Yutong Lin, Yue Cao, Han Hu, Yixuan Wei, Zheng Zhang, Stephen Lin, and Baining Guo. 2021. Swin transformer: Hierarchical vision transformer using shifted windows. In *ICCV*.
- [33] Mingsheng Long, Yue Cao, Jianmin Wang, and Michael I Jordan. 2015. Learning transferable features with deep adaptation networks. In *ICML*. 97–105.
- [34] Mingsheng Long, Yue Cao, Jianmin Wang, and Philip S Yu. 2016. Composite correlation quantization for efficient multimodal retrieval. In *SIGIR*. 579–588.
- [35] Mingsheng Long, Zhangjie Cao, Jianmin Wang, and Michael I Jordan. 2018. Conditional adversarial domain adaptation. In *NeurIPS*. 1647–1657.
- [36] Mingsheng Long, Han Zhu, Jianmin Wang, and Michael I Jordan. 2017. Deep Transfer Learning with Joint Adaptation Networks. In *ICML*. 2208–2217.
- [37] Muzammal Naseer, Kanchana Ranasinghe, Salman Khan, Fahad Shahbaz Khan, and Fatih Porikli. 2022. On improving adversarial transferability of vision transformers. In *CVPR*.
- [38] Anh Nguyen, Jason Yosinski, and Jeff Clune. 2015. Deep neural networks are easily fooled: High confidence predictions for unrecognizable images. In *CVPR*. 427–436.
- [39] Poojan Oza, Vishwanath A Sindagi, Vibashan VS, and Vishal M Patel. 2021. Unsupervised domain adaptation of object detectors: A survey. *CoRR,abs/2105.13502* (2021).
- [40] Sinno Jialin Pan and Qiang Yang. 2010. A survey on transfer learning. *TKDE* 22, 10 (2010), 1345–1359.
- [41] Xingchao Peng, Qinxun Bai, Xide Xia, Zijun Huang, Kate Saenko, and Bo Wang. 2019. Moment Matching for Multi-Source Domain Adaptation. In *ICCV*. 1406–1415.
- [42] Xingchao Peng, Ben Usman, Neela Kaushik, Judy Hoffman, Dequan Wang, and Kate Saenko. 2017. Visda: The visual domain adaptation challenge. *CoRR,abs/1710.06924* (2017).
- [43] Maithra Raghu, Thomas Unterthiner, Simon Kornblith, Chiyuan Zhang, and Alexey Dosovitskiy. 2021. Do Vision Transformers See Like Convolutional Neural Networks?. In *NeurIPS*.
- [44] Subhankar Roy, Aliaksandr Siarohin, Enver Sangineto, Samuel Rota Bulo, Nicu Sebe, and Elisa Ricci. 2019. Unsupervised domain adaptation using feature-whitening and consensus loss. In *CVPR*. 9471–9480.
- [45] Changjian Shui, Zijian Li, Jiaqi Li, Christian Gagné, Charles X Ling, and Boyu Wang. 2021. Aggregating from multiple target-shifted sources. In *ICML*. 9638–9648.
- [46] Baochen Sun, Jiashi Feng, and Kate Saenko. 2016. Return of frustratingly easy domain adaptation. In *AAAI*. 2058–2065.
- [47] Zhiqing Sun, Shengcao Cao, Yiming Yang, and Kris M Kitani. 2021. Rethinking transformer-based set prediction for object detection. In *ICCV*. 3611–3620.
- [48] Hugo Touvron, Matthieu Cord, Matthijs Douze, Francisco Massa, Alexandre Sablayrolles, and Hervé Jégou. 2021. Training data-efficient image transformers distillation through attention. In *ICML*. 10347–10357.
- [49] Hemanth Venkateswara, Jose Eusebio, Shayok Chakraborty, and Sethuraman Panchanathan. 2017. Deep hashing network for unsupervised domain adaptation. In *CVPR*. 5018–5027.
- [50] Vedran Vukotić, Christian Raymond, and Guillaume Gravier. 2016. Multimodal and crossmodal representation learning from textual and visual features with bidirectional deep neural networks for video hyperlinking. In *MM Workshops*. 37–44.
- [51] Wenhui Wang, Enze Xie, Xiang Li, Deng-Ping Fan, Kaitao Song, Ding Liang, Tong Lu, Ping Luo, and Ling Shao. 2021. Pyramid vision transformer: A versatile backbone for dense prediction without convolutions. In *ICCV*. 568–578.
- [52] Junfeng Wen, Russell Greiner, and Dale Schuurmans. 2020. Domain aggregation networks for multi-source domain adaptation. In *ICML*. 10214–10224.
- [53] Zhirong Wu, Yuanjun Xiong, Stella X Yu, and Dahua Lin. 2018. Unsupervised feature learning via non-parametric instance discrimination. In *CVPR*. 3733–3742.
- [54] Shaoan Xie, Zibin Zheng, Liang Chen, and Chuan Chen. 2018. Learning semantic representations for unsupervised domain adaptation. In *ICML*. 5423–5432.
- [55] Tongkun Xu, Weihua Chen, Pichao Wang, Fan Wang, Hao Li, and Rong Jin. 2022. CDTrans: Cross-domain Transformer for Unsupervised Domain Adaptation. In *ICLR*.
- [56] Guanglei Yang, Hao Tang, Zhun Zhong, Mingli Ding, Ling Shao, Nicu Sebe, and Elisa Ricci. 2021. Transformer-Based Source-Free Domain Adaptation. *CoRR*,

- abs/2105.14138* (2021).
- [57] Xun Yang, Fuli Feng, Wei Ji, Meng Wang, and Tat-Seng Chua. 2021. Deconfounded video moment retrieval with causal intervention. In *SIGIR*. 1–10.
- [58] Li Yuan, Qibin Hou, Zihang Jiang, Jiashi Feng, and Shuicheng Yan. 2021. Volo: Vision outlooker for visual recognition. *CoRR, abs/2106.13112* (2021).
- [59] Zhang, W., Xu, D., Ouyang, W., and W. Li. 2020. Self-Paced Collaborative and Adversarial Network for Unsupervised Domain Adaptation. *TPAMI* (2020), 1–1.
- [60] Sicheng Zhao, Xiangyu Yue, Shanghang Zhang, Bo Li, Han Zhao, Bichen Wu, Ravi Krishna, Joseph E Gonzalez, Alberto L Sangiovanni-Vincentelli, Sanjit A Seshia, et al. 2020. A review of single-source deep unsupervised visual domain adaptation. *TNNLS* (2020).
- [61] Sixiao Zheng, Jiachen Lu, Hengshuang Zhao, Xiatian Zhu, Zekun Luo, Yabiao Wang, Yanwei Fu, Jianfeng Feng, Tao Xiang, Philip HS Torr, et al. 2021. Rethinking semantic segmentation from a sequence-to-sequence perspective with transformers. In *CVPR*. 6881–6890.
- [62] Yang Zou, Zhiding Yu, B V K Vijaya Kumar, and Jinsong Wang. 2018. Unsupervised Domain Adaptation for Semantic Segmentation via Class-Balanced Self-Training. In *ECCV*. 289–305.